JOURNAL OF CLINICAL MICROBIOLOGY, May 2006, p. 1755–1762 Vol. 44, No. 5
0095-1137/06/$08.00+0 doi:10.1128/JCM.44.5.1755–1762.2006

Human Papillomavirus Type 16 Integration in Cervical Carcinoma In Situ and in Invasive Cervical Cancer

Hugo Arias-Pulido,[1] Cheri L. Peyton,[1]† Nancy E. Joste,[2] Hernan Vargas,[3,4]‡ and Cosette M. Wheeler[1]*

Departments of Molecular Genetics and Microbiology[1] and Department of Pathology,[2] University of New Mexico, Health Sciences Center, School of Medicine, Albuquerque, New Mexico; Grupo Farmacogenética del Cáncer, Dep. Farmacia, Universidad Nacional de Colombia, Bogotá, Colombia[3]; and Grupo de Biología Molecular Tumoral, Instituto Nacional de Cancerología, Bogotá, Colombia[4]

Received 24 October 2006/Returned for modification 5 January 2006/Accepted 20 February 2006

Integration of human papillomavirus type 16 (HPV-16) into the host DNA has been proposed as a potential marker of cervical neoplastic progression. In this study, a quantitative real-time PCR (qRT-PCR) was used to examine the physical status of HPV-16 in 126 cervical carcinoma in situ and 92 invasive cervical cancers. Based on criteria applied to results from this qRT-PCR assay, HPV-16 was characterized in carcinoma in situ cases as episomal (61.9%), mixed (i.e., episomal and integrated; 29.4%), and integrated (8.7%) forms. In invasive cervical cancer samples, HPV-16 was similarly characterized as episomal (39.1%), mixed (45.7%), and integrated (15.2%) forms. The difference in the frequency of integrated or episomal status estimated for carcinoma in situ and invasive cervical cancer cases was statistically significant ($P = 0.003$). Extensive mapping analysis of HPV-16 E1 and E2 genes in 37 selected tumors demonstrated deletions in both E1 and E2 genes with the maximum number of losses (78.4%) observed within the HPV-16 E2 hinge region. Specifically, deletions within the E2 hinge region were detected most often between nucleotides (nt) 3243 and 3539. The capacity to detect low-frequency HPV-16 integration events was highly limited due to the common presence and abundance of HPV episomal forms. HPV-16 E2 expressed from intact episomes may act in trans to regulate integrated genome expression of E6 and E7.

With about 400,000 new cases and nearly 250,000 deaths each year, cervical cancer contributes significantly to worldwide cancer-related morbidity and mortality (37). In the United States, approximately 11,000 new cases of invasive cervical cancer (CC) were expected in 2004, and approximately 4,000 women would die of the disease (12). Epidemiologic studies have shown that low-grade squamous intraepithelial lesions (LSIL) and high-grade squamous intraepithelial lesions (HSIL) present different genetic as well as viral characteristics that, under certain circumstances, give cells an advantage to progress to more severe lesions and CC (21, 30). Further, epidemiologic and molecular evidence is sufficient to conclude that high-risk human papillomaviruses (HPVs), specifically HPV types 16 and 18 (HPV-16 and -18), are etiologic agents for CC (39). In the majority of cases, however, most HPV-associated lesions regress spontaneously (21), indicating that additional genomic alterations may also be necessary for progression to cancer.

HPV-16 integration into the host genome has been suggested as a step associated with neoplastic progression. In vitro studies have demonstrated that cell populations with integrated HPV-16 posses a selective growth advantage compared to cells that maintain HPV-16 viral genomes as episomes (13, 14, 27). This growth advantage is thought to result from disruption of the HPV-16 E2 open reading frame, which may lead to increased cell immortalization capacity by augmenting the steady-state levels of mRNAs encoding the viral oncogenes E6 and E7 (14, 27). HPV-16 integration has been reported with different frequencies in all spectrums of cervical neoplasias from LSIL (6, 7, 24, 32) to HSIL and CC (2, 4, 8, 10, 11, 15–18, 23, 24, 29, 31, 34–36, 40, 41). In general, the frequency of HPV-16 viral integration increased in parallel with the severity of cervical lesions. These reports have suggested that viral integration could represent a risk for tumor progression (7, 8, 10, 11, 17, 24, 32, 34). In addition, HPV-16 integration has been associated with poor clinical outcome (16, 35, 36).

The purpose of this study was to examine the physical status of HPV-16 in a set of carcinomas in situ (CIS) and CC tumors and map the specific viral integration sites when possible. Towards this end, a previously reported quantitative real-time PCR (qRT-PCR) was applied based on the assumption that the quantitative ratio of HPV-16 E2 to E6 gene targets would allow discrimination of the physical status of HPV-16 (24).

MATERIALS AND METHODS

Clinical specimens and cell lines. A total of 166 HPV-16-positive tumor biopsies representing formalin-fixed, paraffin-embedded specimens from 126 CIS and 40 CC cases comprised part of the material. The tissues were obtained from a New Mexico population-based study, and the characterization of a portion of the population and HPV status has been published elsewhere (25). In addition, 52 HPV-16-positive tumor biopsies derived from patients diagnosed with invasive cervical cancer at the National Cancer Institute in Bogotá, Colombia, were also analyzed (26). All samples were provided without patient identifiers. The studies were approved by local internal review boards.

Paraffin-embedded tissue microdissection and processing. Tumor cells from paraffin-embedded tissue specimens were microdissected as described by Arias-

* Corresponding author. Mailing address: Department of Molecular Genetics and Microbiology, School of Medicine, Health Sciences Center, University of New Mexico, Albuquerque, NM 87111. Phone: (505) 272-5785. Fax: (505) 277-0265. E-mail: cwheeler@salud.unm.edu.

† Present address: Department of Zoology, Oregon State University, Corvallis, Oreg.

‡ Present address: Grupo Farmacogenética del Cáncer, Dep. Farmacia, Universidad Nacional de Colombia, Bogotá, Colombia.

TABLE 1. Primers used for mapping HPV-16 E1 and E2 genes and detection of beta-globin target regions

Primer	5′ to 3′ sequence	Location[a]	Size (bp)
E1F1	CAGGTACCAATGGGGAAGA	878–896	
E1R1	ACCTGTACTGCATCTCTATGTTGT	1095–1118	241
E1F2	GACAGCACATGCGTTGTTTAC	1059–1079	
E1R2	AGTCTCATGGCGCCCTTC	1306–1323	265
E1F3	CGCCATGAGACTGAAACAC	1312–1330	
E1R3	GAAAAACTCACCCCGTATAAC	1503–1523	212
E1F4	GTTATACGGGGTGAGTTTTTC	1503–1523	
E1R4	ATCATCATACACATTGGAGACA	1763–1784	282
E1F5	GTGTGTCTCCAATGTGTATGATG	1760–1782	
E1R5	GCAATTTCACTATCGTCTACTATG	1968–1991	232
E1F6	GGGCCTACGATAATGACATAGTA	1952–1974	
E1R6	TGCTTCCAATCACCTCCAT	2168–2186	235
E1F7	GGAGGTGATTGGAAGCAA	2170–2187	
E1R7	CCAATGCATTTCTTAAATTGTC	2464–2485	316
E1F8	CCCTGTTGGAACTACATAGATGAC	2443–2466	
E1R8	CCTCGTCCTCGTGCAAACT	2725–2743	301
E1F9	CCAGTGTATGAGCTTAATGATAAGA	2662–2686	
E2R9	GTCTATATGGTCACGTAGGTCTGTA	2824–2848	187
E2F10	GTGTGTCAGGACAAAATACTAACA	2783–2806	
E2R10	AAATACACTTCAAGGCTAACGTC	3041–3063	281
E2F11	GAAAAGTGGACATTACAAGACGTTA	3023–3047	
E2R11	CTGCACAAAATATGTTCGTATTC	3243–3265	243
E2F12	GAATACGAACATATTTTGTGCAG	3243–3265	
E2R12	CTGAGTCTCTGTGCAACAACTTA	3517–3539	297
E2F13	CTAAGTTGTTGCACAGAGACTCA	3516–3538	
E2R13	GACGACACTGCAGTATACAATGTAC	3681–3705	190
E2F14	CATGGCATTGGACAGGACATA	3708–3728	
E5R14	ACGCCAGTAATGTTGTGGAT	3870–3889	182
PCO3	ACACAACTGTGTTCACTAGC	62150–62169	
PCO4	CAACTTCATCCACGTTCACC	62240–62259	110
Probe	TAACGGCAGACTTCTCCTCAGGAGTCAGG	62195–62223	
GlobF	GATGCCCTCTCTCACCACTC	71147–71166	
GlobR	AATGGTCATACTGCCCAAGG	71609–71619	473
E6FqPCR	GAGAACTGCAATGTTTCAGGACC	94–115	
E6RqPCR	TGTATAGTTGTTTGCAGCTCTGTGC	150–174	81
E6 Probe	CAGGAGCGACCCAGAAAGTTACCACAGTT	119–147	
E2FqPCR	AACGAAGTATCCTCTCCTGAAATTATTAG	3362–3390	
E2RqPCR	CCAAGGCGACGGCTTTG	3427–3443	82
E2 Probe	CACCCCGCCGCGACCCATA	3407–3425	

[a] Nucleotide positions based on the revised, or HPV-16R, sequence (20, 22) and GenBank accession no. U01317 for beta-globin. Primers used to detect HPV-16 E6 and E2 by qPCR were described elsewhere (24).

Pulido et al. (1). Briefly, cells were isolated by manual microdissection after toluidine blue staining (0.05% [wt/vol]), and normal and tumor DNA from each individual specimen was crudely extracted by digestion with proteinase K (10 mM Tris, 1 mM EDTA [pH 8.5], proteinase K, 0.2 mg/ml, 0.1% Laureth-12) for 24 h at 55°C, followed by proteinase K inactivation at 95°C for 10 min. The cell lysate was diluted 10-fold with water, and 2 μl was used for each amplification reaction.

Fresh tissue and cell line processing. Fresh tumor biopsies (Colombian samples) were snap-frozen in liquid nitrogen and stored at −80°C immediately following a clinical examination. All frozen specimens used in the study were determined to contain at least 80% tumor cells by hematoxylin and eosin staining. Tumor DNA was obtained as previously described (26). Briefly, DNA from tumor samples and cell lines was isolated using standard procedures of proteinase K digestion, phenol-chloroform extraction, and ethanol precipitation. Tumor and cell line DNAs were quantitated using Pico Green (Molecular Probes, Eugene, OR).

SiHa (HPV-16-positive) and C-33A (HPV-negative) cell lines were obtained from the American Tissue Culture Collection. The SiHa cell line contains one to two copies per cell of HPV-16 and presents a disruption of the E2 open reading frame at the 3134–3384 region as a result of viral integration into the host genome (19). The W12 cell line was kindly provided by M. A. Stanley (Department of Pathology, University of Cambridge, United Kingdom). At low passage levels, W12 cells stably maintain HPV-16 replicons at a copy number of approximately 1,000 copies per cell (13). In our laboratory we measured HPV-16 episomes in W12 cells by qRT-PCR and detected on average of between 1×10^3 and 5×10^3 copies of HPV-16 per cell.

Detection of HPV-16 physical status.(i) qRT-PCR. Real-time PCR for HPV-16 E2 and E6 was performed as described elsewhere (24) except that the E6 and E2 probes were labeled with 6-carboxyfluorescein at the 5′ end and 6-carboxytetramethylrhodamine at the 3′ end (Sigma-Genosys, The Woodlands, TX). The sequences of these primers are provided in Table 1. The qRT-PCR was performed with the GeneAmp 5700 sequence detection system (Applied Biosystems, Foster City, CA). Briefly, a standard PCR was carried out in a 50-μl reaction volume containing 1× PCR GeneAmp PCR gold buffer supplemented with 3.0 mM $MgCl_2$ (Applied Biosystems, Foster City, CA), 0.2 mM deoxynucleotide triphosphates, 2 μl of the cell lysate (1 to 5 ng of DNA in the case of purified tumor DNA), and 1 unit of AmpliTaq DNA polymerase (Applied Biosystems, Foster City, CA). The amplification conditions were 2 min at 50°C, 10 min at 95°C, and a two-step cycle of 95°C for 15 s and 60°C for 60 s for a total of 40 cycles. The final primer and probe concentrations, in a total volume of 50 μl, were 0.3 and 0.1 mM, respectively. The DNA quality of each specimen was assessed by a separate qRT-PCR for beta-globin using the forward (PCO3) and reverse (PCO4) primers shown in Table 1. The PCR conditions were the same as for the HPV-16 E6 and E2 genes, except the concentration of Mg was 4 mM and a total of 50 cycles were used.

For each set of samples analyzed, a standard curve was obtained by amplification of HPV-16 plasmid using a 10-fold dilution series (1×10^4 to 1×10^0 copies). The standard curve was used to extrapolate the copy numbers of selected

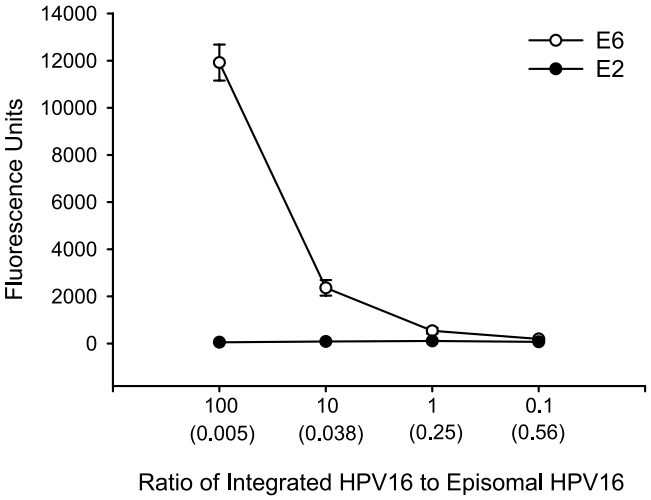

FIG. 1. Detection threshold of the HPV-16 qRT-PCR assay. Values in fluorescence units for the E6 and E2 gene targets are shown on the *y* axis. The ratio of integrated HPV (SiHa) to episomal HPV-16 (W12) DNA in each reaction is shown on the *x* axis. Below the *x* axis scale in parentheses is the mean ratio derived from E6:E2 qRT-PCR values at each defined combination of integrated and episomal forms. SiHa (1×10^4 to 1×10^1 HPV-16 genome equivalents per reaction) was combined with 10^2 genome equivalents of W12. Bars indicate standard errors; open and filled circles indicate individual quantitative PCR values obtained for E6 and E2, respectively (see the text for details).

gene targets present in each clinical specimen. Dilutions were prepared in a background of a crude C-33A cell lysate (1×10^4 cells per reaction). All samples were analyzed in triplicate. In addition, 10-fold dilutions of SiHa (1×10^4 to 1×10^1 HPV-16 genome equivalents per reaction) and W12 cell lysate (1×10^3 to 1×10^1 HPV-16 genome equivalents per reaction) and a no-template control reaction mixture (water) were included in each microplate analysis. Assignment of integrated, mixed or episomal physical status was calculated for each clinical specimen as proposed elsewhere (24). This calculation assumed that E2 and E6 gene segments are present in equivalent proportions within each episomal HPV genome and that integrated HPV genome forms would have the E2 target deleted or absent. Thus, integration was determined by subtracting the copy numbers of E2 (episomal) from the total copy numbers of E6 (episomal and integrated). The ratio of episomal E2 gene target to the integrated E6 gene target represents the amount of the HPV episomal form in relation to the integrated form. Integration was defined by absence of the E2 signal or ratios of 0.001 to 0.003. This ratio cutoff was obtained in reconstitutions experiments when SiHa (integrated form) was in a 10-fold excess of W12 (episomal form) (Fig. 1; also see details in the Results section). Ratios of less than 1 (range, 0.004 to 0.99) indicated the presence of both integrated and episomal forms, and ratios of greater than 1 (range, 1.00 to 7.29) indicated a predominance of episomal forms.

(ii) Deletion mapping of HPV-16 E1/E2 genes by PCR. Fifty-two fresh frozen invasive cervical cancer tumors were used initially to examine the general integrity of HPV-16 E1 and E2 genes by PCR targeting of three larger gene fragments. HPV-16 E1 gene targets were detected by PCR amplification of two segments using overlapping primers E1F1 and E1R5 (1,114 bp) and E1F5 and E2R9 (1,089 bp) (Table 1). A single HPV-16 E2 gene fragment was amplified with primers E1F9 and E2R14 (1,228 bp; Table 1). These PCR fragments were obtained using the Takara LA *Taq* amplification kit (Takara, Madison, WI). Reactions were performed in 50 μl of buffer that contained 2.5 mM $MgCl_2$, 0.2 mM deoxynucleotide triphosphates, 0.5 U LA *Taq* polymerase, and 0.3 μM of each primer. Five cycles of 93°C, 30 s; 55°C, 60 s; and 72°C, 60 s were followed by 37 cycles with the following thermal cycling: 93°C, 30 s; 50°C, 60 s; 72°C, 90 s. All amplicons were visualized on 1.5% agarose gels following staining with ethidium bromide.

Overlapping primer pairs used to more finely map HPV-16 E1 and E2 regions are shown in Table 1. The forward (F) and reverse (R) primers are noted for 14 primer pairs employed. HPV-16 primers were selected in an attempt to achieve HPV type specificity by sequence alignments of all HPV genomes using the MultAli program (3). Subsequently, 10-ng samples of HeLa, SW756 (both HPV-18 positive), ME180 (positive for HPV 68), and C-33A were examined in the PCR. While signals from SiHa and W12 were obtained, no signals were observed in C-33A, HeLa, SW756, or ME180 samples. Optimization of primer conditions was performed with a 10-fold dilution series of SiHa (1×10^3 to 1×10^1 HPV-16 genome equivalents per reaction) and W12 cells (1×10^2 to 1×10^1 HPV-16 genome equivalents per reaction). The PCR conditions allowed detection of approximately 10 HPV-16 genome equivalents from both SiHa and W12 cells with the various primer pairs. Intensities varied slightly when PCR products were analyzed in agarose gels.

Standard PCRs consisted of 1× GeneAmp PCR buffer supplemented with 2.5 mM $MgCl_2$ and 0.001% (wt/vol) gelatin (Applied Biosystems, Foster City, CA), 0.2 mM deoxynucleotide triphosphates, 2 μl of the cell lysate, 30 pmol of each forward and reverse primer, and 0.5 U of AmpliTaq DNA polymerase (Applied Biosystems, Foster City, CA) in a total volume of 50 μl. The amplification conditions were 3 min at 93°C, followed by 45 cycles of 93°C for 1 min, 50°C for 1 min, and 72°C for 2 min. A final extension of 10 min at 72°C was added to complete the PCR. Ten-fold dilutions of SiHa (1×10^2 to 1×10^1 HPV-16 genome equivalents per reaction) and W-12 (1×10^1 to 1×10^0 HPV-16 genome equivalents per reaction) cell lysate reaction mixtures were included in each run as positive controls along with no template (water) and C-33A (1×10^4 cells per reaction) as negative controls. To assess DNA sample quality for this analysis, PCR was carried out for the beta-globin gene target under the same conditions, except that a total of 40 cycles were performed. A fragment of 473 bp beta-globin was obtained with the primers GlobF and GlobR shown in Table 1. PCR products were visualized in agarose gels following staining with ethidium bromide.

(iii) HPV-16 nucleotide position numbering. HPV-16 nucleotide positions and comparisons are based on HPV-16R (22), the sequence revised to include corrections previously reported (20).

Statistical analyses. The Pearson chi-square test was used to test for independence between the physical status of HPV-16 in CIS and CC. *P* values were considered significant if less than 0.05.

RESULTS

Integration status of HPV-16. Reconstitution experiments were performed using W12 and SiHa cell lines to represent different amounts and thus ratios of episomal and integrated forms of HPV-16. The assumption was made that in clinical specimens, integration could be a single event potentially occurring in a background of high levels of episomal HPV-16 DNA. For SiHa, given an estimated one to two HPV-16 integration events per cell, HPV-16 genome equivalents directly approximate the number of SiHa cells assayed. For W12 cells, approximately 1,000 to 5,000 HPV-16 genome equivalents per cell were measured in our studies, which is in relative agreement with previous information (13).

As shown in Fig. 1, ratio values close to zero (median, 0.005; range, 0.001 to 0.006) were obtained only when SiHa (integrated DNA; 1×10^4 HPV-16 genome equivalents) was in 100-fold excess of W12 (episomal DNA; 1×10^2 HPV-16 genome equivalents). A ratio value of 0.038 (range, 0.02 to 0.04) was obtained in mixtures that contained at least 10-fold excess of SiHa. A one-to-one mixture of integrated and episomal HPV-16 forms gave a ratio value of 0.25 (range, 0.15 to 0.41). A ratio value of 0.56 (range, 0.4 to 0.8) was obtained when a 10-fold excess of episomal DNA (10 genome equivalents of HPV-16 integrated forms combined with 100 genome equivalents of HPV-16 episomal forms) was present in the mixture. Experiments were performed in triplicate for each qRT-PCR analysis and repeated at least three times. Similar results were obtained when 1×10^5 to 1×10^0 HPV-16 genome equivalents per reaction of SiHa were combined with 1×10^6 to 1×10^0 HPV-16 genome equivalents per reaction of W12. All possible combinations were examined.

PCR efficiencies for E2 and E6 targets were determined for

each individual microplate assayed by the following calculation (5): $E = 10^{-1/S} - 1$, where E is run efficiency and S is the slope of the generated standard curve. A total of 10 individual assay runs were used to calculate the mean and median efficiency values for each target. The E6 mean efficiency was 100.6, the median was 93.1, and the range was 89 to 115. The E2 mean efficiency was 99.1, the median was 93.1, and the range was 83 to 115. In our study, E6 and E2 were quantitated in triplicate and the coefficient of variation for the assay was less than 29%, which is in agreement with other studies of HPV qRT-PCR assays (6, 9). In this work, we defined integration events only for results that gave ratios of 0.001 to 0.003 or no signals for HPV-16 E2 targets but that were positive for HPV-16 E6 and beta-globin gene targets.

Analysis of HPV-16 physical status by the described qRT-PCR in 126 paraffin-embedded CIS samples showed the presence of episomal forms in 78 (61.9%), mixed (episomal and integrated) forms in 37 (29.4%), and integrated forms in 11 (8.7%) CIS samples. The analysis of the physical status in 40 paraffin-embedded CC showed that 14 (35%), 19 (47.5%), and 7 (17.5%) samples presented the virus in episomal, mixed, and integrated forms, respectively. In 52 fresh-frozen tumors, 22 (42.3%), 23 (44.2%), and 7 (13.5%) were characterized as episomal, mixed, and integrated HPV forms, respectively. Combining results from archival paraffin-embedded and fresh frozen invasive cervical tumors, the HPV-16 episomal, mixed, and integrated forms were found in 36 (39.1%), 42 (45.7%), and 14 (15.2%) tumors, respectively. The difference between HPV-16 genomic forms characterized in CIS and CC was statistically significant ($P = 0.003$).

The microdissected paraffin-embedded tissues were generally positive only for HPV-16 (126 CIS and 40 CC). Coinfections with other HPV types were detected in six samples. HPV-33 ($n = 2$), -35, -45, and -59 were detected as single additional HPV infections. One sample presented coinfection with both HPV-31 and HPV-53. This is consistent with a general clonal origin of cancer and its true precursors. Three, two, and one of the six samples were determined to have HPV-16 in episomal, mixed, and integrated forms, respectively. Four samples in the fresh-frozen tumor series were positive for HPV-31 (mixed), -35 (mixed), -39 (episomal), and -61 (mixed) in addition to HPV-16. One additional sample contained both HPV-39 and HPV-62 (mixed). Given the limited number of HPV coinfections we observed, there was no association of mixed infections with HPV integration.

Extensive mapping analysis of HPV-16 E1 and E2 genes was performed with samples that demonstrated HPV-16 integrated as well as mixed and episomal forms with the qRT-PCR assay. In the representative samples shown in Fig. 2, 35 samples demonstrated deletions that were sometimes accompanied by rearrangement. Two additional samples shown (C29 and C57) had no deletions but contained rearrangements. The pattern of E1 and E2 losses found in 18 paraffin-embedded and 19 fresh-frozen tumors is shown in Fig. 2. This analysis indicated that loss of E2 was more common than losses at E1 in both CIS and CC samples. The 3243–3539 fragment, a region that contains the HPV-16 E2 hinge region, was not detected and was presumed deleted in 29 (78.4%) of 37 samples (Fig. 2). The second most commonly deleted region was located in the N terminus (2783 to 3063) of E2. This deletion was observed in 26 (70.3%) of 37 samples. Nineteen of 37 (51.4%) samples showed losses in the E1 gene region.

No detectable deletions in the full-length HPV-16 E1 and E2 gene fragments were found in 46 (88.5%) and 35 (67.3%) of the 52 fresh-frozen tumors, respectively. Thus, no deletions or potential integration sites were identified in a significant proportion of tumors.

Analysis of rearranged sequences. Possible rearrangements were considered when multiple bands were observed upon gel analysis of PCR amplicons. A few samples demonstrated a complex pattern of integration: losses of single E1/E2 fragments were interspersed with PCR positivity in adjacent E1-E2 regions (samples C22, C49, C96, 111, 124, i256, and 266) (Fig. 2). Sequence analyses were conducted on four samples (C28, C29, C34, and C57) with presumed rearrangements located within the primer pair E1F9-E2R14. A fragment of 583 bp was isolated with this primer pair from C28, C29, and C57 samples. A fragment of 520 bp was obtained with this primer pair for C34. Alignment of the HPV-16 reference clone sequence demonstrated no HPV-16 similarities for the 520-bp fragment generated from specimen C34. However, a fragment that consisted of two HPV-16 segments that were head-to-tail linked was reconstructed for C28, C29, and C57 (Fig. 3).

DISCUSSION

Several studies reported in this journal (23, 24, 40) have suggested that detection of HPV-16 integration status through evaluating the HPV-16 E6/E2 ratio is a sensitive method that might be useful in assessing cervical cancer risk. Given the inter- and intra-assay variations in qRT-PCR (6, 9) and the fact that HSIL are often surrounded by LSIL containing a high copy number of HPV episomal forms (28), we believed that use of this technique may not be readily amenable to routine detection of HPV-16 integration. We conducted reconstitution experiments to assess the sensitivity of the assay. In our hands, this method allowed distinction of integrated versus episomal HPV-16 DNA only when integrated forms were in 100-fold excess of episomal DNA forms. A 10-fold excess of integrated viral DNA above the episomal form gave values close to 0 (range, 0.02 to 0.04), and a slight decrease in the copy number of integrated viral DNA shifted the values, which by this assay would indicate the presence of mixed forms (i.e., both integrated and episomal forms) of HPV-16 (Fig. 1). Similar results have been reported that suggested a lack of sensitivity of the assay examined here (23).

In spite of these observations, we attempted to apply this technique to assess the physical status of HPV-16 in cervical tumors. Review of the literature indicates the presence of both integrated and episomal HPV genomic forms in cervical cancers, but the extent of this phenomenon is unclear. Analysis of the viral status using the qRT-PCR assay showed that, in general, exclusively integrated HPV-16 genomes were detectable as an infrequent event in both CIS (8.7%) and CC (15.2%) microdissected tumors. Instead, episomal and mixed forms were commonly detected. Analyses using microdissected paraffin-embedded samples versus DNA from fresh tissues showed that the frequencies of episomal (35.0% versus 42.3%), mixed (47.5% versus 44.2%), and integrated (17.5% versus 13.5%) forms of HPV-16 were similar by this assay. As ex-

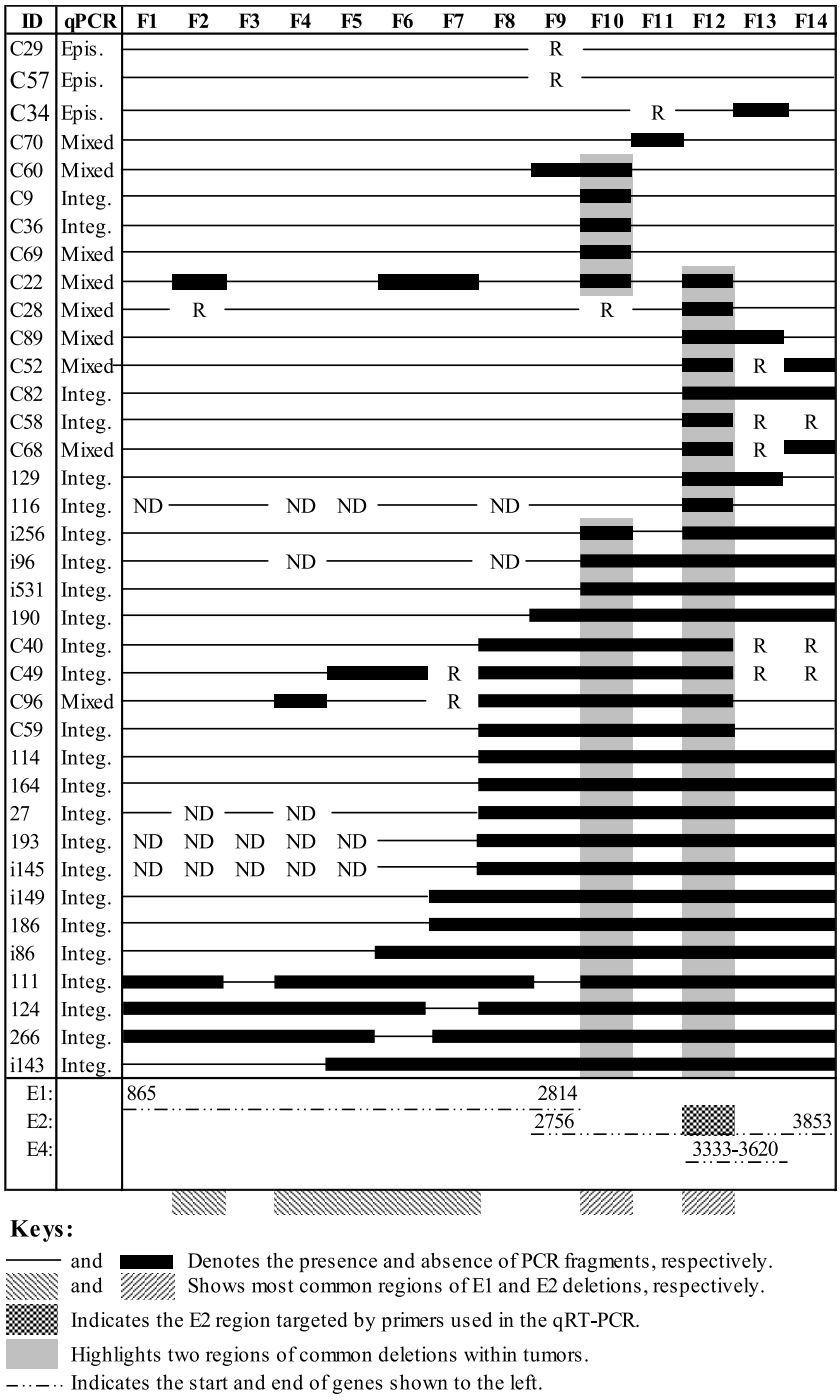

FIG. 2. Deletion mapping of HPV-16 E1 and E2 genes in CIS and CC samples. Selected samples demonstrating E1 and E2 losses ($n = 35$) and two tumors containing rearrangements with no losses (C29 and C57) are included. ID column indicates individual specimen identifiers; fresh frozen cervical tumors are designated by C followed by numeric assignments; paraffin-embedded specimens are denoted by numeric assignments with no alpha modifier for CIS and the addition of an i preceding the number for invasive CC tumors; qPCR column designates integrated, episomal, and mixed forms based on E2:E6 ratio determinations. Various columns indicated by F represent the upstream primer for each pair specified in Table 1. R, rearrangements detected by gel analysis; ND, not determined.

pected, our results suggest that the E2/E6 qRT-PCR assay was not able to commonly detect HPV-16 integration events even in microdissected, tumor-enriched populations of cells. This is presumably due to the common presence of HPV-16 episomal forms in the majority of cervical cancers. In addition, the existence of deletions outside of the proposed E2 target and the presence of concatemers that, though integrated, still conserve intact copies of the E2 gene could mask the detection of integration in some samples.

Mapping analyses of E1 and E2 amplicons demonstrated

FIG. 3. Rearrangements in HPV-16 E2 sequences. A. Nucleotide positions per HPV-16R sequence are noted at the top of the sequence information and correspond to nucleotide positions 2690 to 2870 and 3469 to 3871. The 17 nucleotides that serve as the recombination site are shown in italics. B. Illustration of the proposed end-joining recombination event shown here as an example in tumor C28 that leads to reconstruction of the 583-bp fragment obtained.

the extent of deletions outside of the E2 region targeted by the qRT-PCR assay. In addition, a few cases demonstrated a complex pattern of deletions, suggesting the presence of rearranged HPV-16 sequences (Fig. 2). Rearrangements of HPV-16 sequences have been previously described, but no attempt to characterize the involved regions was made (15, 33, 41). Because short identical nucleotides (up to 10 bases) at the viral and cellular sites seem to facilitate viral integration, it has been suggested that nonhomologous end-joining recombination may occur in vivo (41). We isolated and identified in three samples a 17-bp fragment that could potentially allow recombination of HPV fragments by this mechanism (Fig. 3). It is interesting that this short segment is found in the two regions that showed the highest integration frequency in all samples analyzed: the first location is at nucleotides 2854 to 2870, a region covered by primers E2F10 and E2R10, and the second location is at nucleotides 3452 to 3468, a region targeted by primers E2F12 and E2R12 (Fig. 3). Whether the 17-nucleotide sequence is involved in sequence-specific viral recombination events, such as those consistent with molecular "baiting" (38), remains unknown. Further systematic studies of both E1 and E2 and cellular integration junctions are warranted.

Loss of E1 and E2 open reading frame upon HPV-16 integration in cervical lesions and cancer has been reported in several studies (2, 4, 8, 10, 11, 15–18, 23, 24, 29, 31, 34–36, 40, 41). We found in our study that integration occurred more frequently in the E2 gene. Specifically, the E2 hinge region, targeted by primers E2F12 and E2R12 (nt 3243 to 3539), was deleted in 78.4% of 37 selected samples, followed by deletions in 67.6% of specimens in the region covered by primers E2F10 and E2R10 (nt 2783 to 3063). Although HPV-16 integration has been found in both the E1 and E2 genes, a "hot" spot has not been described. Reports have varied considerably on the frequencies and sites of viral integration identified, which may be explained by differences in technical approaches employed or by differences in the populations studied.

A close review of the few published systematic analyses of HPV-16 integration demonstrated that the E2 region 3132 to 3599, which includes the regions examined in our study, was deleted in ~60% tumors (16, 29, 36), and it was also deleted in a high percentage of cervical intraepithelial neoplasia I to cervical intraepithelial neoplasia III lesions (29). A second region, 2738 to 3189, which includes our most commonly deleted region targeted by E2F10 and E2R10, was also found to be deleted in ~71% of tumors (16, 36). These studies were performed in tumors derived from populations with different ethnic backgrounds. Our study includes samples from two different populations, from the United States and Colombia. We found that the E2F10-E2R10 (2783 to 3063) and the E2F12-E2R12 (3243 to 3539) regions are deleted in 25 (67.6%) tumors and 29 (78.4%) of 37 tumors, respectively. Our data therefore support the existence of a hot spot for HPV-16 viral integration that may be present in a majority of cervical tumors regardless of the ethnic background of the population studied.

A systematic study of E1 deletions has not been previously reported. One group reported that a common region of deletion was found close to the segment encompassed by primers E1F6 and E1R6 (nt 1952 to 2186), followed by deletions in regions flanked by primers E1F4 to E1R7 (nt 1503 to 2485) (18, 41) (Fig. 2). These integration sites were also found in a few of our samples (Fig. 2).

The suggestion that methodologies employed to detect HPV-16 integration may be responsible for the reported discrepancies is consistent with the higher detection of integration events in cervical cancer using more sensitive techniques (15, 17). For example, Kalantari et al., using a system aimed at specifically detecting integrated forms of HPV-16, reported integration in 14 (70%) of 20 samples that previously were reported as containing episomal forms (15). Higher frequencies (88%) of HPV-16 integration in CC have been described with a method based on amplification of transcripts (17).

The role of HPV-16 integration in cervical neoplastic progression has been proposed from studies that demonstrated that disruption of HPV-16 E2 releases the repressor activities of this gene product on HPV-16 E6 and E7 genes. This in turn could lead to an increase in the expression levels of HPV-16 E6 and E7 oncogenes, conferring a growth advantage on the affected cells (13, 14, 27). Our results, however, showed that HPV-16 integration events exist in the presence of hundreds to thousands of viral episomes and that strict viral integration occurs in a low percentage of CIS and CC tumors. This observation suggests that HPV-16 E2 may often be available in *trans* to modulate or regulate HPV-16 E6 and E7 expression. After performing experi-

ments using a W12 culture model of cervical carcinogenesis, Pett et al. recently reported that loss of inhibitory high-risk HPV episomes is required for the spontaneous selection of cells containing integrated HPV-16 (24a). Extant data and current dogma must be given serious reconsideration.

ACKNOWLEDGMENTS

We thank V. V. V. S. Murty for providing the HeLa, SW756, and ME180 DNA, E.-M. de Villiers for kindly providing the HPV-16 reference plasmid, Curtis Hunt for assistance with statistical analyses, Michelle Ozbun for propagating and preparing the W12 cells used as controls, and the gynecologists from the Department of Gynecology at the INC (Colombia).

This work was supported by a RAC grant, C-2239-T, to H.A.-P., and an NIH grant, AI32917, to C.M.W. Support from Colciencias (Colombia) (grant 2101-04-11896) is also acknowledged.

REFERENCES

1. **Arias-Pulido, H., N. Joste, and C. Wheeler.** 2004. Loss of heterozygosity on chromosome 6 in HPV-16 positive cervical carcinomas carrying the DRB1*1501-DQB1*0602 haplotype. Genes Chromosomes Cancer **40:**277–284.
2. **Berumen, J., E. Unger, L. Casas, and P. Figueroa.** 1995. Amplification of human papillomavirus types 16 and 18 in invasive cervical cancer. Hum. Pathol. **26:**676–681.
3. **Corpet, F.** 1988. Multiple sequence alignment with hierarchical clustering. Nucleic Acids Res. **16:**10881–10890.
4. **Daniel, B., A. Rangarajan, G. Mukherjee, E. Vallikad, and S. Krishna.** 1997. The link between integration and expression of human papillomavirus type 16 genomes and cellular changes in the evolution of cervical intraepithelial neoplastic lesions. J. Gen. Virol. **78:**1095–1101.
5. **Fink, L., W. Seeger, L. Ermert, J. Hanze, U. Stahl, F. Grimminger, W. Kummer, and R. M. Bohle.** 1998. Real-time quantitative RT-PCR after laser-assisted cell picking. Nat. Med. **4:**1329–1333.
6. **Fontaine, J., C. Hankins, M. Mayrand, J. Lefevre, D. Money, S. Gagnon, A. Rachlis, K. Pourreaux, A. Ferenczy, and F. Coutlee.** 2005. High levels of HPV-16 DNA are associated with high-grade cervical lesions in women at risk or infected with HIV. AIDS **19:**785–794.
7. **Gallo, G., M. Bibbo, L. Bagella, A. Zamparelli, F. Sanseverino, M. R. Giovagnoli, A. Vecchione, and A. Giordano.** 2003. Study of viral integration of HPV-16 in young patients with LSIL. J. Clin. Pathol. **56:**532–536.
8. **Graham, D. A., and C. S. Herrington.** 2000. HPV-16 E2 gene disruption and sequence variation in CIN 3 lesions and invasive squamous cell carcinomas of the cervix: relation to numerical chromosome abnormalities. Mol. Pathol. **53:**201–206.
9. **Gravitt, P., C. Peyton, C. Wheeler, R. Apple, R. Higuchi, and K. Shah.** 2003. Reproducibility of HPV 16 and HPV 18 viral load quantitation using TaqMan real-time PCR assays. J. Virol. Methods **112:**23–33.
10. **Hopman, A., F. Smedts, W. Dignef, M. Ummelen, G. Sonke, M. Mravunac, G. Vooijs, E. Speel, and F. Ramaekers.** 2004. Transition of high-grade cervical intraepithelial neoplasia to micro-invasive carcinoma is characterized by integration of HPV 16/18 and numerical chromosome abnormalities. J. Pathol. **202:**23–33.
11. **Hudelist, G., M. Manavi, K. I. D. Pischinger, T. Watkins-Riedel, C. F. Singer, E. Kubista, and K. F. Czerwenka.** 2004. Physical state and expression of HPV DNA in benign and dysplastic cervical tissue: different levels of viral integration are correlated with lesion grade. Gynecol. Oncol. **92:**873–880.
12. **Jemal, A., R. C. Tiwari, T. Murray, A. Ghafoor, A. Samuels, E. Ward, E. J. Feuer, and M. J. Thun.** 2004. Cancer statistics, 2004. CA Cancer J. Clin. **54:**8–29.
13. **Jeon, S., B. Allen-Hoffmann, and P. Lambert.** 1995. Integration of human papillomavirus type 16 into the human genome correlates with a selective growth advantage of cells. J. Virol. **69:**2989–2997.
14. **Jeon, S., and P. Lambert.** 1995. Integration of human papillomavirus type 16 DNA into the human genome leads to increased stability of E6 and E7 mRNAs: implications for cervical carcinogenesis. Proc. Natl. Acad. Sci. USA **92:**1654–1658.
15. **Kalantari, M., E. Blennow, B. Hagmar, and B. Johansson.** 2001. Physical state of HPV16 and chromosomal mapping of the integrated form in cervical carcinomas. Diagn. Mol. Pathol. **10:**46–54.
16. **Kalantari, M., F. Karlsen, G. Kristensen, R. Holm, B. Hagmar, and B. Johansson.** 1998. Disruption of the E1 and E2 reading frames of HPV 16 in cervical carcinoma is associated with poor prognosis. Int. J. Gynecol. Pathol. **17:**146–153.
17. **Klaes, R., S. M. Woerner, R. Ridder, N. Wentzensen, M. Duerst, A. Schneider, B. Lotz, P. Melsheimer, and M. V. K. Doeberitz.** 1999. Detection of high-risk cervical intraepithelial neoplasia and cervical cancer by amplification of transcripts derived from integrated papillomavirus oncogenes. Cancer Res. **59:**6132–6136.
18. **Luft, F., R. Klaes, M. Nees, M. Durst, V. Heilmann, P. Melsheimer, and M. von Knebel Doeberitz.** 2001. Detection of integrated papillomavirus sequences by ligation-mediated PCR (DIPS-PCR) and molecular characterization in cervical cancer cells. Int. J. Cancer **92:**9–17.
19. **Meissner, J.** 1999. Nucleotide sequences and further characterization of human papillomavirus DNA present in the CaSki, SiHa and HeLa cervical carcinoma cell lines. J. Gen. Virol. **80:**1725–1733.
20. **Meissner, J.** 1997. Sequencing errors in reference HPV clones, p. III-110–III-123. *In* G. Myers, C. Baker, K. Munger, F. Sverdup, A. McBride, H.-U. Bernard, and J. Meissner (ed.), Human papillomaviruses 1997: a compilation and analysis of nucleic acid and amino acid sequences. Theoretical biology and biophysics. Los Alamos National Laboratory, Los Alamos, N.M.
21. **Melnikow, J., J. Nuovo, A. Willan, B. Chan, and L. Howell.** 1998. Natural history of cervical squamous intraepithelial lesions: a meta-analysis. Obstet. Gynecol. **92:**727–735.
22. **Myers, G., H.-U. Bernard, H. Delius, C. Baker, J. Icenogle, A. Halpern, and C. Wheeler.** 1995. Human papillomavirus. A compilation and analysis of nucleic acid and amino acid sequences. Publication LA-UR 95–3675. Los Alamos National Laboratory, Los Alamos, N.M.
23. **Nagao, S., M. Yoshinouchi, Y. Miyagi, A. Hongo, J. Kodama, S. Itoh, and T. Kudo.** 2002. Rapid and sensitive detection of physical status of human papillomavirus type 16 DNA by quantitative real-time PCR. J. Clin. Microbiol. **40:**863–867.
24. **Peitsaro, P., B. Johansson, and S. Syrjanen.** 2002. Integrated human papillomavirus type 16 is frequently found in cervical cancer precursors as demonstrated by a novel quantitative real-time PCR technique. J. Clin. Microbiol. **40:**886–891.

24a. **Pett, M. R., M. T. Herdman, R. D. Palmer, G. S. H. Yeo, M. K. Shivji, M. A. Stanley, and N. Coleman.** 2006. Selection of cervical keratinocytes containing integrated HPV16 associates with episome loss and an endogenous antiviral response. Proc. Natl. Acad. Sci. USA **103:**3822–3827.

25. **Peyton, C., P. Gravitt, W. Hunt, R. Hundley, M. Zhao, R. Apple, and C. Wheeler.** 2001. Determinants of genital human papillomavirus detection in a US population. J. Infect. Dis. **183:**1554–1564.
26. **Pulido, H. A., M. J. Fakruddin, A. Chatterjee, E. D. Esplin, N. Beleno, G. Martinez, H. Posso, G. A. Evans, and V. V. V. S. Murty.** 2000. Identification of a 6-cM minimal deletion at 11q23.1–23.2 and exclusion of PPP2R1B gene as a deletion target in cervical cancer. Cancer Res. **60:**6677–6682.
27. **Romanczuk, H., and P. Howley.** 1992. Disruption of either the E1 or the E2 regulatory gene of human papillomavirus type 16 increases viral immortalization capacity. Proc. Natl. Acad. Sci. USA **89:**3159–3163.
28. **Sherman, M. E., S. S. Wang, C. M. Wheeler, L. Rich, P. E. Gravitt, R. Tarone, and M. Schiffman.** 2003. Determinants of human papillomavirus load among women with histological cervical intraepithelial neoplasia 3: dominant impact of surrounding low-grade lesions. Cancer Epidemiol. Biomarkers Prev. **12:**1038–1044.
29. **Stevenson, M., L. C. Hudson, J. E. Burns, R. L. Stewart, M. Wells, and N. J. Maitland.** 2000. Inverse relationship between the expression of the human papillomavirus type 16 transcription factor E2 and virus DNA copy number during the progression of cervical intraepithelial neoplasia. J. Gen. Virol. **81:**1825–1832.
30. **Stoler, M.** 2000. Human papillomaviruses and cervical neoplasia: a model for carcinogenesis. Int. J. Gynecol. Pathol. **19:**16–28.
31. **Terry, G., L. Ho, and J. Cuzick.** 1997. Analysis of E2 amino acid variants of human papillomavirus types 16 and 18 and their associations with lesion grade and HLA DR/DQ type. Int. J. Cancer **73:**651–655.
32. **Tonon, S., M. Picconi, P. Bos, J. Zinovich, J. Galuppo, L. Alonio, and A. Teyssie.** 2001. Physical status of the E2 human papilloma virus 16 viral gene in cervical preneoplastic and neoplastic lesions. J. Clin. Virol. **21:**129–134.
33. **Tornesello, M. L., F. M. Buonaguro, L. Buonaguro, I. Salatiello, E. Beth-Giraldo, and G. Giraldo.** 2000. Identification and functional analysis of sequence rearrangements in the long control region of human papillomavirus type 16 Af-1 variants isolated from Ugandan penile carcinomas. J. Gen. Virol. **81:**2969–2982.
34. **Ueda, Y., T. Enomoto, T. Miyatake, K. Ozaki, T. Yoshizaki, H. Kanao, Y. Ueno, R. Nakashima, K. Shroyer, and Y. Murata.** 2003. Monoclonal expansion with integration of high-risk type human papillomaviruses is an initial step for cervical carcinogenesis: association of clonal status and human papillomavirus infection with clinical outcome in cervical intraepithelial neoplasia. Lab. Investig. **83:**1517–1527.
35. **Unger, E., S. Vernon, W. Thoms, R. Nisenbaum, C. Spann, I. Horowitz, J. Icenogle, and W. Reeves.** 1995. Human papillomavirus and disease-free survival in FIGO stage Ib cervical cancer. J. Infect. Dis. **172:**1184–1190.
36. **Vernon, S., E. Unger, D. Miller, D. Lee, and W. Reeves.** 1997. Association of human papillomavirus type 16 integration in the E2 gene with poor disease-free survival from cervical cancer. Int. J. Cancer **74:**50–56.
37. **Vizcaino, A., V. Moreno, F. Bosch, N. Munoz, X. Barros-Dios, J. Borras, and D. Parkin.** 2000. International trends in incidence of cervical cancer: II. Squamous-cell carcinoma. Int. J. Cancer **86:**429–435.

38. **Wentzensen, N., S. Vinokurova, and M. V. K. Doeberitz.** 2004. Systematic review of genomic integration sites of human papillomavirus genomes in epithelial dysplasia and invasive cancer of the female lower genital tract. Cancer Res. **64:**3878–3884.
39. **World Health Organization.** 2005. IARC Monographs on the evaluation of carcinogenic risks to humans, vol. 90. Human papillomaviruses. International Agency for Research on Cancer, Lyon, France.
40. **Yoshinouchi, M., A. Hongo, K. Nakamura, J. Kodama, S. Itoh, H. Sakai, and T. Kudo.** 1999. Analysis by multiplex PCR of the physical status of human papillomavirus type 16 DNA in cervical cancer. J. Clin. Microbiol. **37:**3514–3517.
41. **Ziegert, C., N. Wentzensen, S. Vinokurova, F. Kisseljov, J. Einenkel, M. Hoeckel, and M. von Knebel Doeberitz.** 2003. A comprehensive analysis of HPV integration loci in anogenital lesions combining transcript and genome-based amplification techniques. Oncogene **22:**3977–3984.